



A *neo*-pentyl-ferrocene motif for the synthesis of electroactive polyesters

C. John McAdam*, Stephen C. Moratti, Brian H. Robinson, Jim Simpson

Department of Chemistry, University of Otago, P.O. Box 56, Dunedin 9054, New Zealand

ARTICLE INFO

Article history:

Received 2 April 2008

Received in revised form 7 May 2008

Accepted 13 May 2008

Available online 22 May 2008

Keywords:

Ferrocenyl

Polyester

Side-chain

Electrochemistry

Crystal structure

ABSTRACT

Several new *neo*-pentylenediol based ferrocenyl molecules have been prepared using Friedel–Crafts acylation and Clemmensen reduction techniques. The acyl or methyl linker by which the ferrocenyl group is attached tunes the redox properties of the small molecule. The X-ray crystal structure of the acylferrocene with protecting ester groups, its derivative dialcohol, and the methylferrocene dialcohol compounds are reported. Melt polymerisation conditions result in an elimination from the acyl monomer, but a mild carbodiimide coupling protocol successfully generates a number of *neo*-pentylenediol/aromatic dicarboxylate polyesters with pendant ferrocenyl groups.

© 2008 Elsevier B.V. All rights reserved.

1. Introduction

The first ferrocene-containing macromolecule, poly(vinylferrocene), made a low-key debut in 1955 [1]. In the late 1960s however, interest in ferrocene polymers burgeoned [2], and the impetus established continues today due to a recognition of the unique physical and chemical properties the incorporation of an organometallic component offers when compared with conventional organic polymers [3]. The use of metallopolymers in a diverse range of applications, which exploit the combination of polymer processability and metal centre derived functionality, have been comprehensively reviewed [4]. The two main architectures available for ferrocenyl-containing polymers are main-chain polymers, in which the metallocene is incorporated into the backbone, and side-chain polymers, where it is attached in some way to a polymer backbone [5,6]. There are numerous examples known of ferrocene-containing polyesters with main-chain incorporation based on 1,1'-ferrocenedicarboxylic acid (Fig. 1a) [7–11]. Polyesters with pendant ferrocenyl groups, however, are limited to malonyl [12,13] and succinyl [14,15] motifs (Fig. 1b and c). The importance of polyesters in contemporary life [16], and an apparent void in the literature, provided the inspiration for the present paper in which we present new ferrocenyl substituted *neo*-pentyl diols (Fig. 1d) suitable for polyester synthesis.

2. Results and discussion

Synthesis of the ferrocenyl monomers are outlined in Scheme 1. All compounds were characterised by ¹H and ¹³C NMR, IR and UV/Vis spectroscopy, elemental analysis and mass spectroscopy. The precursor 2,2-bis-(hydroxymethyl)propionic acid (bis-MPA) was acetylated and converted to its acyl chloride [17]. This was converted to the new compound **1** by the Friedel–Crafts acylation of ferrocene using standard methodology [18,19]. Both steps gave a relatively low yield (10–20%) compared with typical ferrocenyl acylations. This is possibly the result of competition between the desired electrophilic attack of the acylium cation on ferrocene, and an intra-molecular attack on the acetyl groups used to protect the alcohol functionalities of the bis-MPA. Use of an alternative silyl protecting group not susceptible to electrophilic attack is the subject of current work. Addition of Amberlite IRA 401 resin (OH⁻ form) to a methanol solution of **1** removed the protecting acetyl groups to give the *neo*-pentyl diol **2**. Numerous synthetic attempts were made to improve the yield of **1**. Inexplicably, workup of one of these reactions resulted in the isolation of some deacetylated products (**2** and the half protected compound **2b**). Another previously unreported compound **2c** was also isolated from several of the IRA 401/MeOH deprotection batches. The *neo*-pentyl acyl compounds were orange crystalline solids. Infrared spectroscopy showed a strong ferrocenyl carbonyl stretch 1644–1648 cm⁻¹, and for the compounds with protecting groups (**1** and **2b**), the anticipated acetyl C=O stretch at higher energy. Electronic and NMR spectra are again typical of acylferrocenes with a weak band in the visible region around 460 nm ($\epsilon \sim 400$), and predicted shifts and multiplicities in

* Corresponding author. Tel.: +64 34797920; fax: +64 34797906.
E-mail address: mcadamj@chemistry.otago.ac.nz (C.J. McAdam).

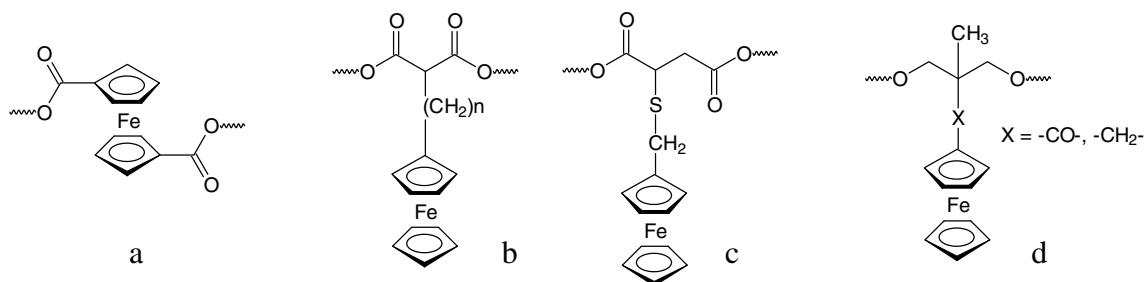
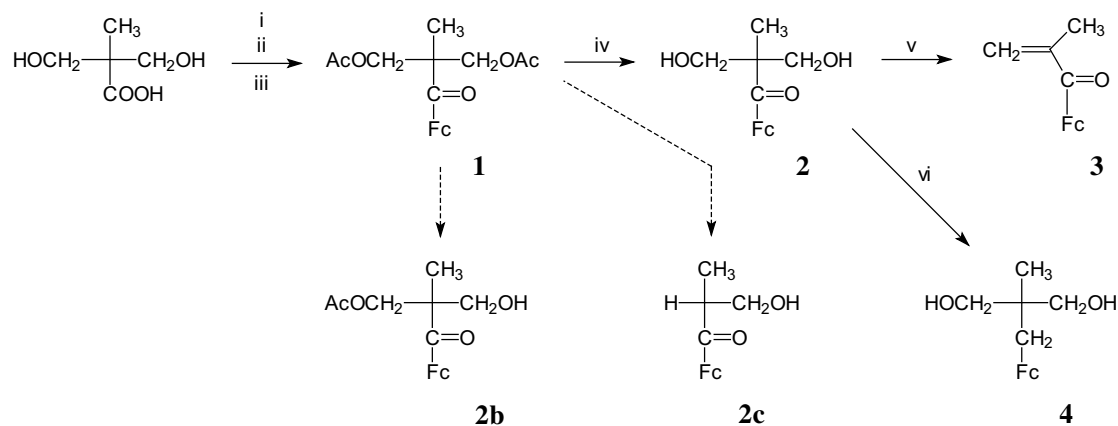


Fig. 1.



Scheme 1. (i) CH_3COCl , NEt_3 , DMAP, CH_2Cl_2 ; (ii) oxalyl chloride, DMF, CH_2Cl_2 ; (iii) FcH, AlCl_3 , CH_2Cl_2 ; (iv) IRA 401, MeOH; (v) calcium acetate, Δ ; (vi) Zn/HgBr_2 , HBr, EtOH.

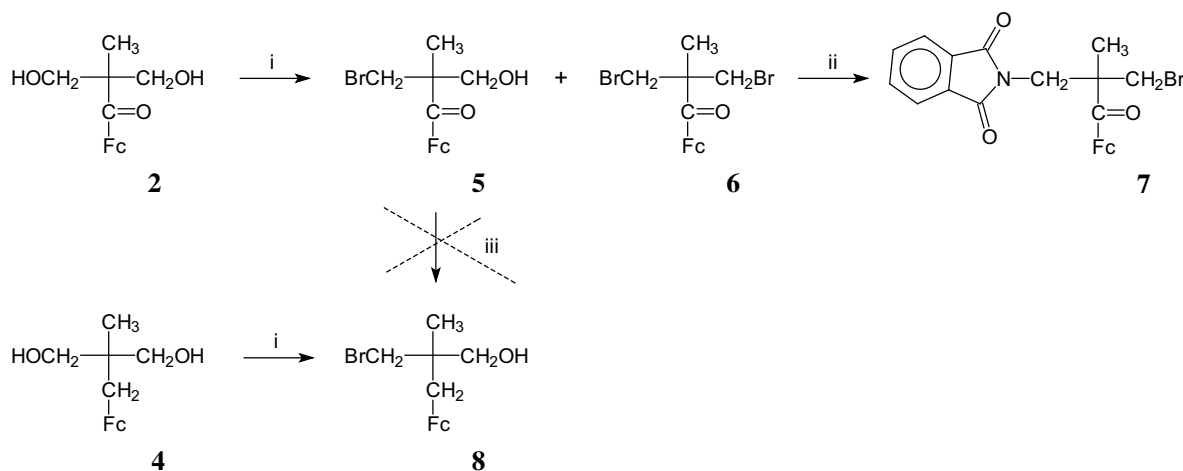
proton and carbon NMR. In the ferrocenyl *iso*-butyl ketone derivative **2c** the C=O stretch in the infrared spectrum drops to 1636 cm^{-1} , presumably the result of intra-molecular hydrogen bonding to the adjacent CH_2OH . The protons of the substituted cyclopentadienyl ring are magnetically inequivalent generating a distinctive set of α , α' , β , β' multiplets in accord with the asymmetric nature of the *iso*-butyl appendage.

The synthesis of poly(ethylene terephthalate) (PET) involves two ester exchange reactions [20]. The first of these is transesterification between dimethyl terephthalate and an excess of ethylene glycol at $150\text{ }^\circ\text{C}$. A second transesterification under vacuum and at further elevated temperature results in elimination of glycol and drives the reaction to form the polyester chain. This methodology avoids the requirements of strict stoichiometric balance and is carried out in the presence of calcium acetate and antimony trioxide as ester exchange and polymerisation catalysts. By analogy, a sample of dimethyl terephthalate and an excess of the substituted propylene glycol **2** were heated to $150\text{ }^\circ\text{C}$ with calcium acetate and antimony trioxide ester catalysts. Instead of an ester exchange, the reaction generated methacryloylferrocene **3** [21] consistent with an elimination of formaldehyde and water from **2**. To avoid the acylferrocene's proclivity to elimination, it was reduced using a Clemmensen reduction to give the methylferrocene compound **4** (Scheme 1), a yellow crystalline solid. The visible spectrum was typical of an alkylferrocene, with the ferrocenyl d-d band observed at slightly higher energy and lower intensity (λ_{max} 442 nm , $\epsilon \sim 130$) than the acyl precursor. Its NMR spectrum was similarly typical of a methylferrocene, and as to be expected the C=O stretch absorption band is absent from its IR spectrum. All the small molecules described had good solubility in common aromatic, chlorocarbon and polar solvents.

2.1. Diamine analogues

Following the successful synthesis of the diol monomers, attempts were made to derivatise these to analogous diamines as possible precursors for polyamides. The strategy for this involved conversion of the alcohol functionalities to halide followed by a Gabriel synthesis, an approach used successfully in this laboratory for the preparation of other ferrocenyl amines [22]. The reaction of **2** with *N*-bromosuccinimide (NBS)/ PPh_3 [23] gave the mono- and dibrominated compounds **5** and **6** in 35% and 20% yields, respectively (Scheme 2). This prevalence of the mono over bis substitution and the low overall yield proved problematic in this and subsequent reactions. The first step of the Gabriel synthesis is the conversion of the halide to phthalimide in DMSO as solvent. Reaction of the dibromo derivative **6** gave the mixed phthalimido/bromo compound **7** in 10% yield. Also present was the methacryloylferrocene elimination product (**3**) and traces of unreacted dibrominated precursor, but no evidence of any diphtalimido product. Results from a Clemmensen reduction of the acyl group of **5** were inconclusive; however, the mixed bromo/alcohol methylferrocene compound **8** was synthesised in 41% from the NBS/ PPh_3 reaction of **4**. This appeared susceptible to oxidation during (and after) workup and was characterised on the basis of mass spectrometry and ^1H NMR results. No traces of a dibromo methylferrocene analogue of **6** were isolated. The products **5–7** obtained were orange crystalline or oily solids. Spectral properties were similar to the analogous acylferrocenes **1** and **2** and are listed in Section 4.

The prevalence of mono- over disubstitution in each of the above sequences is a result of the slow rate of $\text{S}_{\text{N}}2$ reaction for the *neo*-pentyl group. As the strategy outlined for preparation of the diamines relied on a series of consecutive double nucleophilic substitutions, the law of diminishing returns proved particularly



Scheme 2. (i) NBS, PPh₃, THF; (ii) potassium phthalimide, DMSO; (iii) Zn/HgBr₂, HBr, EtOH.

telling. Other conversion schemes for an alcohol to an amine (e.g. through the azide) still rely on a nucleophilic substitution of the *neo*-pentyl core and thus are likely to suffer from the same limitations. Amines are also prepared by reductive amination, but the susceptibility of the ferrocenyl component of **2** and particularly **4** to oxidation precludes the conversion of the diol molecules to the necessary precursor aldehydes. We conclude that the diol monomers are unsuitable for conversion to analogous diamine polyamide precursors by currently available methods.

2.2. X-ray structures of **1**, **2** and **4**

X-ray crystallography confirmed the identification of, and provided structural information for the diester (**1**) and dialcohol molecules (**2**) and (**4**).

The structure of **1** comprises a ferrocenyl group substituted on one cyclopentadiene (Cp) ring with the carbonyl group of a *neo*-pentanoyl diacetate. In **2**, the diacetate is hydrolysed to the corresponding diol, while in the diol, **4**, the carbonyl group that links to the ferrocenyl is reduced to a methylene. Bond lengths and angles in all three compounds, Table 1, show normal values [24].

In **1**, (Fig. 2) the ketone carbonyl group lies approximately in the plane of the substituted Cp ring with the O5–C5–C6–C10 angle 1.4(3)° and an rms deviation of only 0.0228 Å from the plane incor-

porating the nine atoms of C2 through to the Cp (C2/C1/C5/O5/C6–C10). This plane in turn is orthogonal to the C3/C1/C4 plane with a dihedral angle of 89.44(9)°. The Cp rings of the ferrocene are close to eclipsed, twist angle 5.6(4)° [25], and coplanar {dihedral angle 1.31(17)°}. At first glance the structure of **2** (Fig. 3) shows a similar orientation of the ferrocene to the *neo*-pentyl ketone as that observed for **1**. However, closer examination shows significantly more deviation from planarity with the O5–C5–C6–C10 torsion angle of –8.92(19)° and C1–C5–C6–C7 –17.6(2)°, and a dihedral angle of 12.76(8)° between the substituted Cp ring plane and that containing atoms O5/C5/C1/C2. This plane remains close to orthogonal to the C3/C1/C4 plane, 87.84(5)°. In the parent 2,2-bis(hydroxymethyl)propionic acid [26], the corresponding dihedral angle is 88.7°. In **2**, the angle between the ferrocenyl ring planes is 4.26(9)° and the rings are somewhat less eclipsed with a twist angle of 11.8(3)°. The crystal structure of the methylferrocene **4** (Fig. 4) adopts a significantly different conformation to that of **1** and **2**. While the *neo*-pentyl unit retains the orthogonality between the C3/C1/C4 and C2/C1/C5 planes, with a dihedral angle of 89.95(7)°, the C2/C1/C5 plane subtends an angle of 70.31(6)° with the substituted Cp ring plane. The unsubstituted Cp ring of the ferrocene is disordered over two positions with an occupancy factor 0.887(4) for the major disorder component. The C atoms of the major component are approximately staggered with respect to those of the substituted Cp ring with a twist angle of 29.2(3)°. In the minor component, the Cp rings are approximately eclipsed, twist angle 2.5(7)°. In both disorder components, the ferrocenyl rings are reasonably coplanar with interplanar angles 0.68(10)° and 2.3(7)° for major and minor respectively. In the acylferrocenes **1** and **2** intramolecular C–H...O hydrogen bonds generate S(5) ring motifs [27] but there is no equivalent interaction in methyl Fc derivative **4**. A similar intra-molecular bonding motif appears in the parent bis-MPA molecule [26].

If the packing interactions that are inevitably present in the solid state are discounted (perhaps an unreasonable expectation even in solution for small molecules with two hydroxyl groups), the O2–C2...C3–O3 torsion angles for the three molecules give an indication of the inherent linearity or twist of a repeat unit that may form on polymerisation; thus a 180° torsion would favour extended systems while smaller angles may predispose the formation of oligomeric and/or cyclic systems. The O2–C2...C3–O3 torsion angles increase from 95.81(9)° for **2** to a more open 112.27(9)° in **4** reflecting the different spatial requirements of the acyl- and methylferrocene units. The diester **1** provides a model of an individual repeat unit that might be expected from polymerisation of **2**. In this case, the O2–C2...C3–O3 torsion angle

Table 1
Selected bond lengths and angles for **1**, **2** and **4**

	1	2	4
Bond lengths (Å)			
C1–C2	1.535(2)	1.5332(17)	1.5380(16)
C1–C3	1.529(2)	1.5427(17)	1.5327(16)
C1–C4	1.537(2)	1.5398(18)	1.5311(16)
C2–O2	1.452(2)	1.4288(17)	1.4309(14)
C5–O5	1.224(2)	1.2282(15)	–
C5–C6	1.480(2)	1.4861(17)	1.5008(16)
C6...C10 ring av C–C	1.42(12)	1.431(9)	1.427(3)
C11...C15 ring av C–C	1.418(4)	1.423(3)	1.415(8)
Fe1...(C6–10) av	2.047(7)	2.046(14)	2.050(5)
Fe1...(C11–15) av	2.047(5)	2.048(9)	2.051(2)
Bond angles (°)			
C2–C1–C3	109.87(15)	109.73(10)	110.95(9)
C2–C1–C4	110.28(15)	107.14(10)	110.13(9)
C2–C1–C5	106.94(14)	109.88(10)	105.25(9)
C1–C2–O2	107.43(14)	112.98(11)	113.07(10)
C1–C5–O5	119.21(15)	119.90(11)	–
C1–C5–C6	121.86(15)	120.87(10)	116.13(9)

Table 2
Hydrogen-bond geometry (Å, °) for **1**, **2** and **4**

D–H...A	D–H	H...A	D...A	D–H...A
1				
C2–H2B...O3	0.97	2.50	2.888(2)	103
C12–H12...O21 ⁱ	0.93	2.48	3.357(2)	157
C13–H13...O5 ⁱ	0.93	2.45	3.374(2)	170
C22–H22C...O5 ⁱⁱ	0.96	2.48	3.400(2)	162
C3–H3A...O31 ⁱⁱⁱ	0.97	2.61	3.492(2)	152
C7–H7...O31 ⁱⁱⁱ	0.93	2.52	3.358(2)	150
C22–H22A...O21 ^{iv}	0.96	2.69	3.527(2)	145
Symmetry codes: (i) $x - 1, y, z$; (ii) $x, y + 1, z$; (iii) $-x + 1, -y + 2, -z$; (iv) $-x + 2, -y + 2, -z + 1$				
2				
O3–H3...O2 ⁱ	0.806(9)	1.928(12)	2.7019(13)	161(2)
O2–H2...O3 ⁱⁱ	0.787(9)	1.940(11)	2.6977(14)	162(2)
C7–H7...O5 ⁱⁱⁱ	0.95	2.54	3.4484(16)	159
C3–H3B...O5 ⁱⁱⁱ	0.99	2.61	3.2808(16)	125
C14–H14...O5 ^{iv}	0.95	2.58	3.4632(19)	155
Symmetry codes: (i) $-x + 1, -y, -z + 2$; (ii) $x + 1, y, z$; (iii) $x - 1, y, z$; (iv) $x - 1/2, -y + 1/2, z - 1/2$				
4				
O2–H2...O3 ⁱ	0.77(2)	1.99(2)	2.7323(12)	163(2)
O3–H3...O2 ⁱⁱ	0.74(2)	2.00(2)	2.7326(13)	170(2)
C4–H4A...O2 ⁱⁱⁱ	0.98	2.62	3.4555(15)	144
Symmetry codes: (i) $x, y, z - 1$; (ii) $-x + 1, -y, -z$; (iii) $-x + 2, -y, -z$				

opens to 119.85(13)° while the C22–C21...C31–C32 torsion between acetate residues is opened even further to 124.5°.

The crystal structure of **1** is stabilised by a set of inter-molecular C–H...O hydrogen bonds (Table 2), augmented by a π ... π stacking interaction between the substituted Cp rings of two adjacent mol-

ecules. The alcohol functionality in **2** and **4** offers the possibility of classical hydrogen bonding to stabilise the structure and, in both molecules, classical centrosymmetric dimers form between adjacent molecules *via* O–H...O hydrogen bonds. These are augmented for **2** by weak C–H...O hydrogen bonds and for **4** by C–H... π

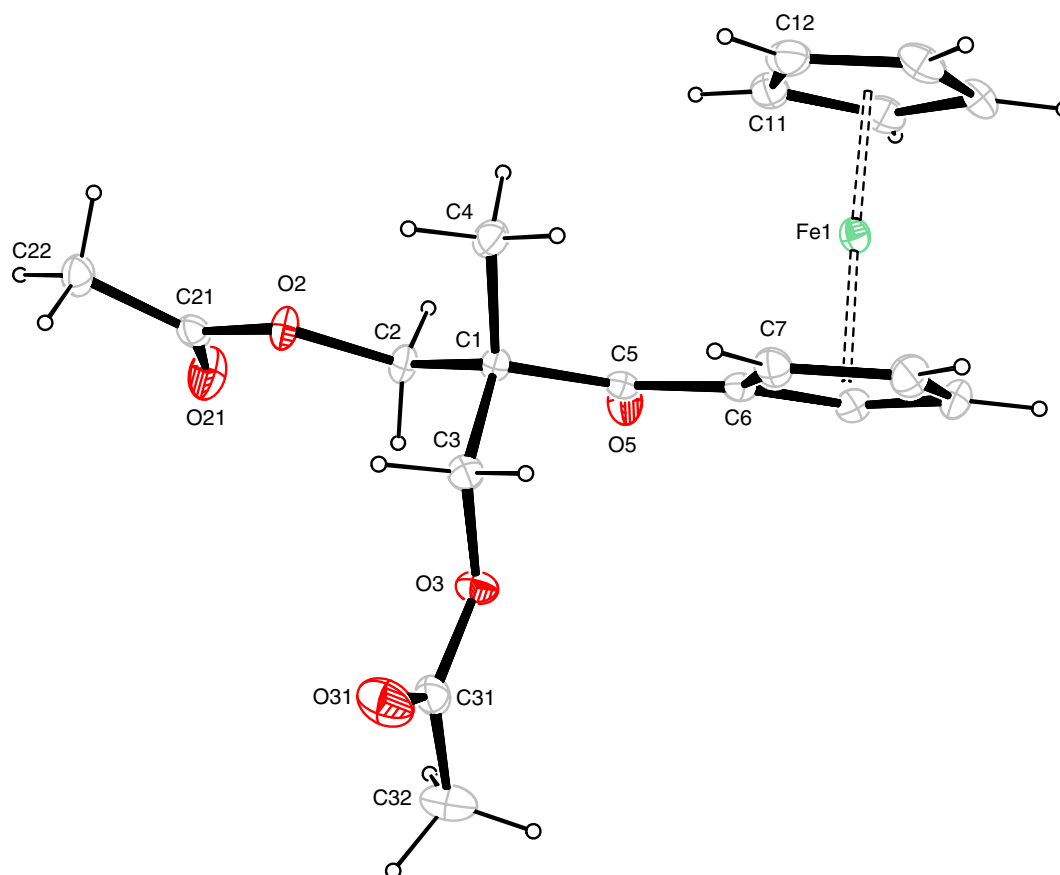


Fig. 2. The molecular structure of **1** showing the atom numbering scheme and with displacement ellipsoids drawn at the 50% probability level. For clarity only the first two C atoms of consecutively numbered cyclopentadienyl ring are numbered.

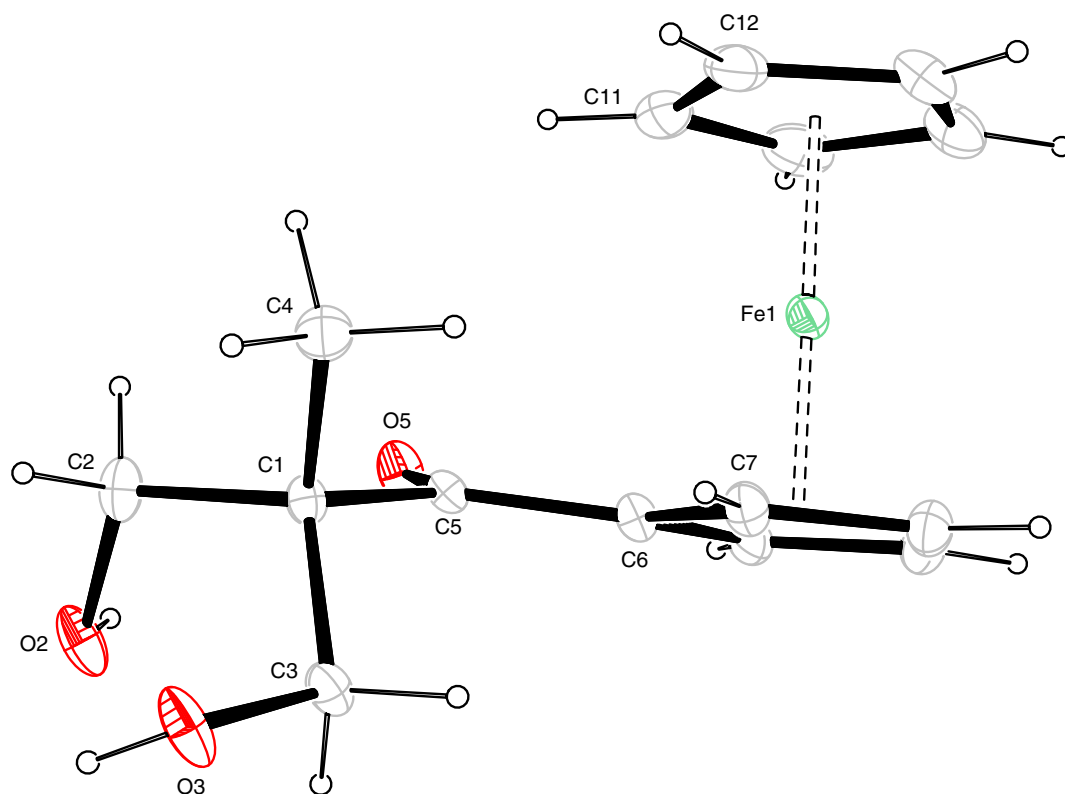


Fig. 3. The molecular structure of **2** showing the atom numbering scheme and with displacement ellipsoids drawn at the 50% probability level. For clarity only the first two C atoms of consecutively numbered cyclopentadienyl ring are numbered.

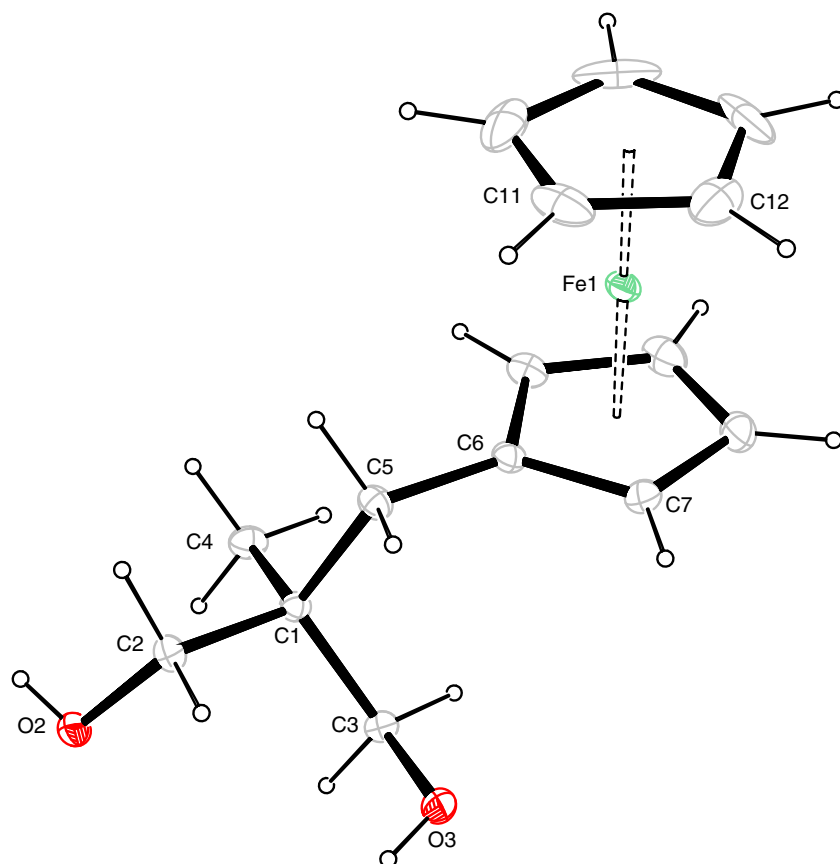


Fig. 4. The molecular structure of the major disorder component of **4** showing the atom numbering scheme and with displacement ellipsoids drawn at the 50% probability level. For clarity only the first two C atoms of consecutively numbered cyclopentadienyl ring are numbered.

interactions. Further details of the crystal packing and packing diagrams appear in [Supplementary material](#).

2.3. Electrochemistry

Cyclic voltammetry was performed on CH_2Cl_2 solutions of **1–4**. This showed the expected reversible one electron oxidation associated with the ferrocenyl group ([Table 3](#)). For the acyl compounds, this occurred around 0.8 V {vs. decamethylferrocene (Fc^+), $\text{Fc}^{+/0} = 0.55 \text{ V}$ [28]} and is typical of ferrocenyl ketones [29–31]. The ferrocenyl redox couple for the mixed acetate/OH compound **2b** fell between those of the bis-acetate (**1**) and diol (**2**) molecules. In the methylferrocene derivative **4**, the oxidation process showed the anticipated cathodic shift to 0.49 V, a potential typical of those encountered for alkylferrocenes [22,32].

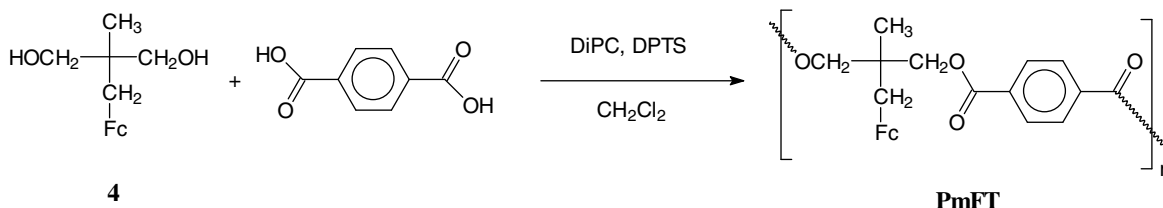
Conceptually, the preparation of polyesters with side-chain ferrocenyl appendages from the diol monomers reported here offers a $\sim 300 \text{ mV}$ variance of redox potential by simple choice of methyl or acyl link to the pendant ferrocenyl group, a result borne out in experiment [33]. There is also the opportunity to tune the redox properties of the pendant ferrocene further by additional substitution (e.g. 2-, 3- or 1'-) either pre- or post-polymerisation.

2.4. Polymerisation

An effective laboratory synthesis of polyesters utilises the method of Moore and Stupp [34]. The carbodiimide based reaction proceeds under mild conditions and without the need for preactivated acid derivatives to generate high molecular weight polymers. Following this protocol the diol monomer **4** was reacted with a series of aryl and aliphatic diacids to generate polyesters with a pendant ferrocenyl group. A representative example, the reaction between **4** and terephthalic acid with diisopropylcarbodiimide (DiPC) and 4-(dimethylamino)pyridinium 4-toluenesulfonate (DPTS) at room temperature to give polymer **PmFT** in $\sim 87\%$ yield, is shown in [Scheme 3](#) and described in Section 4. The mildness of the reaction conditions also allowed the successful polymerisation of the acyl diol monomer **2** which had failed under the more aggressive conditions of the melt polymerisation described above which produced **3**. The polymers formed from **2** and **4** were soluble in toluene and halogenated solvents, but insoluble in MeCN, acetone and simple alcohols. The comprehensive results of the polyester synthesis, characterisation and properties, and an in-depth analysis of monomer and polymer electrochemistry will be

Table 3
Ferrocenyl redox potentials for **1–4** (CH_2Cl_2 , TBAPF₆, referenced against internal decamethylferrocene (Fc^+) for which $[\text{Fc}]^{+/0} = 0.55 \text{ V}$)

	$[\text{Fc}]^{+/0} \text{ (V)}$
1	0.81
2	0.77
2b	0.78
2c	0.79
3	0.80
4	0.49



Scheme 3.

described in future articles [33]. Briefly, however, the polymers formed exhibit spectroscopic properties in accord with their ferrocenyl and aromatic dicarboxylate ester components, and depending on the connecting link involved exhibit a 300 mV variation in the $[\text{Fc}]^{+/0}$ redox process as observed in their respective acyl- or methylferrocene precursor.

3. Conclusions

Two new ferrocenyl containing *neo*-pentyl diols have been prepared. These possess the dual features of chemico-physical properties expected for acyl- and methylferrocenes, and incorporation of a pair of hydroxy groups that make them suitable for esterification into larger assemblies. The reluctance of the *neo*-pentyl core to undergo $\text{S}_{\text{N}}2$ reaction, reflected in poor yields, make the diols unsuitable as precursors for analogous diamines.

4. Experimental

2,2-Bis-(hydroxymethyl)propionic acid (bis-MPA) and ferrocene (Acros and Aldrich, respectively) and other reagents were used as received. 2,2-Bis(acetoxymethyl)propionic acid and its acid chloride derivative were prepared from bis-MPA following the method of Hult et al. [17]. IRA 401 resin was used in the hydroxide form. Solvents were dried and distilled by standard procedures, and all reactions unless stated were performed under nitrogen. Microanalyses were carried out by the Campbell Microanalytical Laboratory, University of Otago. APCI mass spectra were recorded on a Shimadzu LCMS-QP8000 α instrument. IR spectra were recorded on a Perkin-Elmer Spectrum BX FT-IR spectrometer, ^1H and ^{13}C NMR spectra on Varian Unity Inova 300 MHz and 500 MHz spectrometers in CDCl_3 (7.26 ppm) at 25 °C; electronic spectra were recorded on Varian Cary 500 UV-Vis. Band maxima were obtained from convoluted spectra. Cyclic and square wave voltammetry in CH_2Cl_2 were performed using a three-electrode cell with a polished Pt 1 mm disk working electrode; solutions were $\sim 10^{-3} \text{ M}$ in electroactive material and 0.10 M in supporting electrolyte (recrystallised TBAPF₆). Data were recorded on a Powerlab/4sp computer-controlled potentiostat. Scan rates of 0.05–1 V s^{-1} were typically employed for cyclic voltammetry and for square-wave voltammetry, square-wave step heights of 5 mV, a square amplitude of 25 mV with a frequency of 15 Hz. All potentials are referenced to decamethylferrocene (Fc^+) [35]; $E_{1/2}$ for sublimed ferrocene was 0.55 V. Molecular weights (M_w and M_n) of polymers were determined by Gel Permeation HPLC using a Jasco PU-960 Intelligent HPLC pump with 20 μl loop, Shodex KF-803 column, and Jasco 830-RI Intelligent RI detector. Polystyrene standards (Fluka), 1 mg/ml in THF, and the polymer samples, 2 mg/ml in THF, were eluted with THF at a flow rate of 1 ml/min. The data were analysed with Cirrus GPC software version 3.1.

4.1. Acylferrocene diester (**1**)

Ferrocene [6.51 g, 35 mmol in CH_2Cl_2 (30 ml)] was added dropwise to a CH_2Cl_2 (60 ml) solution at 0 °C of AlCl_3 (35 mmol) and the

acid chloride prepared from 2,2-bis(acetoxymethyl)propionic acid (35 mmol). The mixture was stirred overnight at room temperature. After quenching with sat. NaCl solution, the organic layer was washed with Na₂CO₃ (10%) solution, dried over MgSO₄ and dried in vacuo. Column chromatography on SiO₂ with CH₂Cl₂ eluted unreacted ferrocene, the orange residue was eluted and rechromatographed with a 2:1 hexane/ethyl acetate combination to give **1**. Concentration of the liquor yielded X-ray quality crystals (2.28 g, 17%).

Anal. Calc. for C₁₉H₂₂FeO₅: C, 59.09; H, 5.74. Found: C, 59.19; H, 5.76%. MS: 387 (MH⁺). ¹H NMR (δ): 4.84 (t, *J* = 1.8 Hz, 2H, Fc α), 4.52 (t, *J* = 1.8 Hz, 2H, Fc β), 4.40 (s, 4H, -CH₂), 4.21 (s, 5H, Fc C₅H₅), 2.04 (s, 6H, acetyl CH₃), 1.40 (s, 3H, -CH₃). ¹³C NMR (δ): 204.6 (Fc-C=O), 170.8 (acetyl C=O), 76.4 (Fc ipso), 72.0 (Fc β), 70.6 (Fc α), 70.0 (C₅H₅), 66.1 (CH₂), 51.0 (C tertiary), 20.9 (acetyl CH₃), 18.9 (CH₃). IR (KBr): ν_{C=O} 1743 (acetyl), 1646 (Fc-C=O) cm⁻¹. UV-Vis (CH₂Cl₂): 337 (1100), 458 (440) nm (ε).

4.2. Acylferrocene diol (**2**)

To a solution of **1** (2.12 g, 5.5 mmol) in MeOH was added Amberlite IRA 401 resin (OH⁻ form) (2.5 g). The mixture was allowed to stand 12 days, after which time a significant quantity of crystalline material was evident in the flask. After evaporation of the solution, the flask contents were redissolved in CH₂Cl₂ and filtered. Column chromatography on SiO₂ with CH₂Cl₂/ethyl acetate 1:1 eluted **2** (1.36 g, 82%). X-ray quality crystals were obtained from CH₂Cl₂/heptane. The product is mobile on SiO₂ with ethyl acetate solvent.

Anal. Calc. for C₁₅H₁₈FeO₃: C, 59.63; H, 6.00. Found: C, 59.43; H, 6.07%. MS: 303 (MH⁺). ¹H NMR (δ): 4.87 (t, *J* = 1.8 Hz, 2H, Fc α), 4.55 (t, *J* = 1.8 Hz, 2H, Fc β), 4.27 (s, 5H, Fc C₅H₅), 4.18, 3.82 [2 × (dd, *J* = 11, 7 Hz, 2H, -CH₂)], 3.34 (t, *J* = 7 Hz, 2H, -OH), 1.20 (s, 3H, -CH₃). ¹³C NMR (δ): 211.0 (Fc -C=O), 76.5 (Fc ipso), 72.1 (Fc β), 70.7 (CH₂), 70.5 (Fc α), 70.2 (C₅H₅), 53.6 (C tertiary), 18.4 (CH₃). IR (KBr): ν_{C=O} 1644 cm⁻¹. UV-Vis (CH₂Cl₂): 347 (1000), 464 (400) nm (ε).

4.2.1. Acylferrocene ester/ol (**2b**)

Isolated during the chromatographic work-up of a batch of **1** (0.40 g, 3%). Anal. Calc. for C₁₇H₂₀FeO₄: C, 59.32; H, 5.86. Found: C, 59.38; H, 6.08%. MS: 345 (MH⁺). ¹H NMR (δ): 4.88 (m, 2H, Fc α), 4.56 (m, 2H, Fc β), 4.61, 4.44 [2 × (d, *J* = 11 Hz, 1H, -CH₂-OAc)], 4.25 (s, 5H, Fc C₅H₅), 3.79, 3.75 [2 × (dd, *J* = 11, 7 Hz, 1H, -CH₂-OH)], 2.75 (t, *J* = 7 Hz, 1H, -OH), 2.08 (s, 3H, acetyl CH₃), 1.37 (s, 3H, -CH₃). ¹³C NMR (δ): 208.2 (Fc -C=O), 171.4 (acetyl C=O), 76.4 (Fc ipso), 72.3, 72.2 (Fc β), 70.1 (C₅H₅), 70.9, 70.6 (Fc α), 66.1 (CH₂), 53.0 (C tertiary), 20.9 (acetyl CH₃), 18.5 (CH₃). IR (KBr): ν_{C=O} 1731 (acetyl), 1648 (Fc -C=O) cm⁻¹.

4.2.2. **2c**

Isolated during the chromatographic work-up of **2** (0.12 g, 8%). Anal. Calc. for C₁₄H₁₆FeO₂: C, 61.79; H, 5.93. Found: C, 61.54; H, 6.04%. MS: 273 (MH⁺). ¹H NMR (δ): 4.86, 4.73 [2 × (m, 1H, Fc α)], 4.55, 4.52 [2 × (m, 1H, Fc β)], 4.24 (s, 5H, Fc C₅H₅), 3.89, 3.74 [2 × (m, 1H, -CH₂)], 3.22 (m, 1H, -CH), 2.65 (t, *J* = 7 Hz, 1H, -OH), 1.22 (d, *J* = 8 Hz, 3H, -CH₃). ¹³C NMR (δ): 208.7 (Fc-C=O), 78.1 (Fc ipso), 72.6, 72.6 (Fc β), 69.9 (C₅H₅), 69.6, 69.4 (Fc α), 64.7 (CH₂), 44.7 (C tertiary), 15.2 (CH₃). IR (KBr): ν_{C=O} 1636 (Fc-C=O) cm⁻¹.

4.3. Methylferrocene diol (**4**)

Compound **2** (0.38 g, 1.26 mmol) was refluxed 2 h in 47% HBr (2.5 ml)/EtOH (26 ml) with an amalgam prepared according to Saji et al. [18] from Zn (2.5 g) and HgBr₂ (0.33 g). The liquor was separated, solvent removed under vacuum, and the CH₂Cl₂ extract

washed with sat. Na₂CO₃. Chromatography (SiO₂) with 1:1 CH₂Cl₂/ethyl acetate gave **4** (0.21 g, 60%). X-ray quality crystals were obtained from slow evaporation of an EtOH solution.

Anal. Calc. for C₁₅H₂₀FeO₂: C, 62.52; H, 7.00. Found: C, 62.79; H, 7.11%. MS: 288 (M⁺). ¹H NMR (δ): 4.10 (s, 5H, Fc C₅H₅), 4.09, 4.06 [2 × (t, *J* = 1.8 Hz, 2H, Fc C₅H₄)], 3.44 (s, 4H, CH₂OH), 2.98 (br s, 2H, -OH), 2.43 (s, 2H, Fc-CH₂), 0.70 (s, 3H, -CH₃). ¹³C NMR (δ): 83.8 (Fc ipso), 70.3 (CH₂), 70.2, 67.7 (C₅H₄), 68.8 (C₅H₅), 40.3 (C tertiary), 35.1 (Fc-CH₂), 19.0 (CH₃). UV-Vis (CH₂Cl₂): 322 sh (140), 442 (130) nm (ε).

4.4. Acylferrocene bromo/ol (**5**) and acylferrocene dibromo (**6**)

N-Bromosuccinimide (0.67 g, 3.75 mmol) and PPh₃ (0.98 g, 3.75 mmol) were added to a solution of **2** (0.45 g, 1.5 mmol) in THF (40 ml) and stirred 3 h. The solvent was removed and the reaction mix separated using column chromatography on SiO₂. CH₂Cl₂ eluent and recrystallisation from CH₂Cl₂/hexane gave orange needles of **6** (0.13 g, 20%). Further elution with a 10:1 CH₂Cl₂/ethyl acetate combination gave **5** (0.19 g, 35%).

Compound **5**: Anal. Calc. for C₁₅H₁₇BrFeO₂: C, 49.35; H, 4.69. Found: C, 49.69; H, 4.91%. MS: 365 (MH⁺). ¹H NMR (δ): 4.85 (t, *J* = 1.8 Hz, 2H, Fc α), 4.57 (t, *J* = 1.8 Hz, 2H, Fc β), 4.24 (s, 5H, Fc C₅H₅), 3.86 (m, 4H, -CH₂), 2.54 (t, *J* = 7 Hz, -OH), 1.46 (s, 3H, -CH₃). IR (KBr): ν_{C=O} 1645 cm⁻¹.

Compound **6**: Anal. Calc. for C₁₅H₁₆Br₂FeO: C, 42.10; H, 3.77. Found: C, 42.32; H, 3.75%. MS: 429 (MH⁺). ¹H NMR (δ): 1.64 (s, 3H, -CH₃), 3.81, 3.92 [2 × (d, *J* = 11 Hz, 2H, -CH₂)], 4.25 (s, 5H, Fc C₅H₅), 4.55 (t, *J* = 1.8 Hz, 2H, Fc β), 4.83 (t, *J* = 1.8 Hz, 2H, Fc α). ¹³C NMR (δ): 203.7 (Fc-C=O), 76.4 (Fc ipso), 72.0 (Fc β), 70.7 (Fc α), 70.3 (C₅H₅), 52.2 (C tertiary), 38.9 (CH₂), 22.7 (CH₃). IR (KBr): ν_{C=O} 1645 cm⁻¹.

4.5. Acylferrocene phthalimido/bromo (**7**)

Compound **6** (0.17 g, 0.4 mmol) and potassium phthalate (0.15 g, 0.8 mmol) were heated in DMSO (10 ml) for 1/2 h. The black solution generated was extracted with CH₂Cl₂ and rinsed with 4 l water. Column chromatography on SiO₂ with CH₂Cl₂ as eluent gave orange **7** (0.02 g, 10%). Due to the low overall yield, this was characterized on the basis of MS, NMR and IR only.

Calc. for C₂₃H₂₀⁷⁹BrFeNO₃: MS: 494 (MH⁺). ¹H NMR (δ): 7.87, 7.75 [2 × (m, 2H, -phthalimide)], 5.01 (m, 2H, Fc α), 4.57 (t, *J* = 1.8 Hz, 2H, Fc β), 4.27 (s, 5H, Fc C₅H₅), 4.23, 4.15 [2 × (d, *J* = 14 Hz, 1H, -CH₂-phthalimide)], 4.00, 3.52 [2 × (d, *J* = 11 Hz, 1H, -CH₂-Br)], 1.59 (s, 3H, -CH₃). ¹³C NMR (δ): 204.1 (Fc-C=O), 168.8 (phthalimide-C=O), 131.9 (phthalimide ipso), 134.4, 123.6 (phthalimide), 77.1 (Fc ipso), 72.1 (Fc β), 70.9 (Fc α), 70.1 (C₅H₅), 54.0 (C tertiary), 43.6 (CH₂-), 39.4 (CH₂-Br), 21.4 (CH₃). IR (KBr): ν_{C=O} 1774, 1716 (phthalimide), 1653 (Fc-C=O) cm⁻¹.

4.6. Methylferrocene bromo/ol (**8**)

Prepared similarly to **5** from the reaction of **4** (0.144 g, 0.5 mmol) with NBS/PPh₃. Flash column chromatography on SiO₂ with CH₂Cl₂ gave a yellow oil **8** (0.07 g, 41%). This proved unstable and was characterized on the basis of MS and ¹H NMR only.

Calc. for C₁₅H₁₉⁷⁹BrFeO: MS: 351 (MH⁺). ¹H NMR (δ): 4.14–4.11, 4.08 [2 × (m, 2H, Fc C₅H₄)], 4.11 (s, 5H, Fc C₅H₅), 3.44, 3.31 [2 × (m, 2H, -CH₂)], 2.48 (m, 2H, Fc-CH₂), 1.46 (t, *J* = 7 Hz, -OH), 0.89 (s, 3H, -CH₃).

4.7. Polymerisation of **4**

Terephthalic acid (0.166 g, 1 mmol) and **4** (0.288 g, 1 mmol) were stirred with diisopropylcarbodiimide (DiPC) (0.505 g,

Table 4
Summary of crystal and structure refinement data for **1**, **2** and **4**

	1	2	4
Empirical formula	C ₁₉ H ₂₂ FeO ₅	C ₁₅ H ₁₈ FeO ₃	C ₁₅ H ₂₀ FeO ₂
Formula weight	386.22	302.14	288.16
Description	Orange plate	Orange block	Yellow plate
Crystal size (mm ³)	0.16 × 0.10 × 0.03	0.19 × 0.07 × 0.07	0.34 × 0.31 × 0.05
T (K)	85(2)	89(2)	91(2)
Crystal system	Triclinic	Monoclinic	Monoclinic
Space group	P $\bar{1}$	P2(1)/n	P2(1)/n
a (Å)	8.4103(3)	5.9277(2)	5.9079(2)
b (Å)	8.4388(4)	16.4708(6)	38.4212(12)
c (Å)	12.7827(6)	13.7274(5)	6.2059(2)
α (°)	80.860(2)	90	90
β (°)	77.952(1)	100.144(2)	112.901(1)
γ (°)	78.453(1)	90	90
V (Å ³)	862.77(7)	1319.31(8)	1297.63(7)
Z	2	4	4
T _{min} , T _{max}	0.814, 0.973	0.816, 0.923	0.755, 0.944
θ (°)	1.64–26.39	3.01–34.09	3.18–32.83
Total reflections	18941	26719	24292
Independent reflections (R _{int})	3525 (0.0398)	4915 (0.0344)	4692 (0.0283)
Reflections with I > 2 σ (I)	3037	4169	4364
Goodness-of-fit on F ²	1.025	1.053	1.138
R ₁ [I > 2 σ (I)]	0.0302	0.0324	0.0315
wR ₂ (all data)	0.0662	0.0867	0.0759
Residuals (e Å ⁻³)	0.455 and -0.287	0.567 and -0.341	0.473 and -0.450

4 mmol) and 4-(dimethylamino)pyridinium 4-toluenesulfonate (DPTS) (1.18 g, 4 mmol) in CH₂Cl₂ (20 ml) at room temperature for 4 days. Purification of the polymer formed was by two precipitations from MeOH to give **PmFT** (0.36 g, 87%).

Anal. Calc. for {C₂₃H₂₂FeO₄}_n: C, 66.05; H, 5.30. Found: C, 66.17; H, 5.92%. M_n 4500, M_w 12000. ¹H NMR (δ): 8.10 (s, 4_nH, -terephthalate), 4.22 (br s, 4_nH, -CH₂), 4.09 (s, 5_nH, Fc C₅H₅), 4.07 (m, 4_nH, Fc C₅H₄), 2.65 (s, 2_nH, Fc-C H₂), 1.07 (s, 3_nH, -CH₃). IR (KBr): $\nu_{C=O}$ 1718; ν_{CO-O} 1269, 1243; ν_{O-C} 1120, 1098 cm⁻¹. UV–Vis (CH₂Cl₂): 324 sh (150), 438 (120) nm (ε).

5. X-ray crystallography

Diffraction data for **1**, **2** and **4** were collected on a Bruker APEXII CCD diffractometer equipped with Mo K α (λ = 0.71073 Å) at 85(2) K, 89(2) and 91 K, respectively. Each crystal was mounted on a mylar loop in a thin film of Paratone N oil. A full sphere of data was collected for each compound using the ω -scan technique. Data were processed with APEX2 V2.0-2 and SAINT V7.23A [36] with multi-scan absorption corrections applied using SADABS [36]. The structure of **1** was solved with SIR97 [37] and those of **2** and **4** with SHELXS [38]. All three were refined using SHELXL [38] and TITAN [39]. A summary of crystallographic data is given in Table 4. Figures were produced using ORTEP-3 for Windows [40] and MERCURY, Version 2.0 [41]. Packing was investigated using MERCURY and PLATON [42] and PARST [43] with CIF files generated using SHELXL and enCIFer [44].

Acknowledgements

We are grateful to the New Zealand Foundation for Research Science and Technology for a Postdoctoral Fellowship to C.J.M., to Campbell Easton and Sophie Gardiner for assistance with synthesis, and the University of Otago for purchase of the diffractometer.

Appendix A. Supplementary material

CCDC 683160, 683161 and 683162 contain the supplementary crystallographic data for this paper. These data can be obtained free of charge from The Cambridge Crystallographic Data Centre via www.ccdc.cam.ac.uk/data_request/cif. Supplementary data associated with this article can be found, in the online version, at doi:10.1016/j.jorganchem.2008.05.019.

References

- [1] F.S. Arimoto, A.C. Haven Jr., J. Am. Chem. Soc. 77 (1955) 6295.
- [2] C.U. Pittman Jr., J. Inorg. Organomet. Polym. Mater. 15 (2005) 33.
- [3] K.E. Gonsalves, X. Chen, in: A. Togni, T. Hayashi (Eds.), Ferrocenes, VCH, Weinheim, 1995, pp. 497–530.
- [4] G.R. Whittell, I. Manners, Adv. Mater. 19 (2007) 3439.
- [5] I. Manners, Synthetic Metal-containing Polymers, Wiley-VCH, Weinheim, 2004.
- [6] R.D.A. Hudson, J. Organomet. Chem. 637–639 (2001) 47.
- [7] V.P. Red'ko, V.K. Skubin, D.F. Kutepov, V.V. Korshak, V.G. Mochalov, Vysokomol. Soedin. B: Kratkie Soobshcheniya 22 (1980) 222.
- [8] A.I. Volozhin, L.Y. Verkhovodka, A.A. Rozmyslova, Y.M. Paushkin, Vysokomol. Soedin. B: Kratkie Soobshcheniya 19 (1977) 593.
- [9] H. Valot, Bull. Soc. Chim. Fr. (1969) 1972.
- [10] A.S. Abd-El-Aziz, E.K. Todd, R.M. Okasha, T.E. Wood, Macromol. Rapid Commun. 23 (2002) 743.
- [11] M.M. Abd-Alla, M.F. El-Zohry, K.I. Aly, M.M. Abd-El-Wahab, J. Appl. Polym. Sci. 47 (1993) 323.
- [12] G. Wilbert, R. Zentel, Macromol. Chem. Phys. 197 (1996) 3259.
- [13] G. Wilbert, S. Traud, R. Zentel, Macromol. Chem. Phys. 198 (1997) 3769.
- [14] C.S. Combs Jr., C.I. Ashmore, Ferrocene polyesters, US Patent No. 3 898 254, 1975.
- [15] C.S. Combs Jr., C.I. Ashmore, Solid propellant having a ferrocene containing polyester fuel binder, US Patent No. 3 886 007, 1975.
- [16] J. Scheirs, T.E. Long (Eds.), Modern Polyesters: Chemistry and Technology of Polyesters and Copolyesters, Wiley, Chichester, 2003.
- [17] H. Ihere, A. Hult, E. Söderlind, J. Am. Chem. Soc. 118 (1996) 6388.
- [18] T. Saji, K. Hoshino, Y. Ishii, M. Goto, J. Am. Chem. Soc. 113 (1991) 450.
- [19] J.-X. Fang, Z. Jin, Z.-M. Li, W. Liu, Appl. Organomet. Chem. 17 (2003) 145.
- [20] W.R. Sorenson, W. Sweeny, T.W. Campbell, Preparative Methods of Polymer Chemistry, 3rd ed., Wiley Interscience, New York, 2001.
- [21] Ö. Dogan, V. Şenol, S. Zeytinci, H. Koyuncu, A. Bulut, J. Organomet. Chem. 690 (2005) 430.
- [22] C.J. McAdam, B.H. Robinson, J. Simpson, Organometallics 19 (2000) 3644.
- [23] A.K. Bose, B. Lal, Tetrahedron Lett. 40 (1973) 3937.
- [24] F.H. Allen, O. Kennard, D.G. Watson, L. Brammer, A.G. Orpen, R. Taylor, J. Chem. Soc., Perkin Trans. 2 (1987) S1.
- [25] The twist angle for all three molecules is defined as the mean C_m–C_{g1}–C_{g2}–C_n torsion angles (C_{g1} and C_{g2} are the centroids of the C₆–C₁₀ and C₁₁–C₁₅ cyclopentadienyl rings, m = 6–10 and n = m + 5).
- [26] G. Müller, J. Lachmann, J. Wunderle, Z. Naturforsch. B: Chem. Sci. 48 (1993) 1299.
- [27] J. Bernstein, R.E. Davis, L. Shimoni, N.-L. Chang, Angew. Chem., Int. Ed. Engl. 34 (1995) 1555.
- [28] F. Barrière, W.E. Geiger, J. Am. Chem. Soc. 128 (2006) 3980.
- [29] N.G. Connelly, W.E. Geiger, Chem. Rev. 96 (1996) 877.
- [30] P. Braunstein, L. Douce, F. Balegroune, D. Grandjean, D. Bayeul, Y. Dusausoy, P. Zanella, New J. Chem. 16 (1992) 925.
- [31] J. Gan, H. Tian, Z. Wang, K. Chen, J. Hill, P.A. Lane, M.D. Rahn, A.M. Fox, D.D.C. Bradley, J. Organomet. Chem. 645 (2002) 168.
- [32] C.J. McAdam, J.L. Morgan, B.H. Robinson, J. Simpson, P.H. Rieger, A.L. Rieger, Organometallics 22 (2003) 5126.
- [33] C.J. McAdam, A.M. Bond, S.C. Moratti, A. Nafady, B.H. Robinson, J. Simpson, in preparation.
- [34] J.S. Moore, S.I. Stupp, Macromolecules 23 (1990) 65.
- [35] I. Noviantri, K.N. Brown, D.S. Fleming, P.T. Gulyas, P.A. Lay, A.F. Masters, L. Phillips, J. Phys. Chem. B 103 (1999) 6713.
- [36] Bruker AXS Inc., APEX2 Version 2.0-2, SAINT Version 7.23A and SADABS 2004/1, Madison, WI, USA, 2006.
- [37] A. Altomare, M.C. Burla, M. Camalli, G.L. Casciarano, C. Giacovazzo, A. Guagliardi, A.G.G. Moliterni, G. Polidori, R. Spagna, J. Appl. Crystallogr. 32 (1999) 115.
- [38] G.M. Sheldrick, Acta Crystallogr., Sect. A 64 (2008) 112.
- [39] K.A. Hunter, J. Simpson, TITAN2000, University of Otago, New Zealand, 1999.
- [40] L.J. Farrugia, J. Appl. Crystallogr. 30 (1997) 565.
- [41] C.F. Macrae, P.R. Edgington, P. McCabe, E. Pidcock, G.P. Shields, R. Taylor, M. Towler, J. van de Streek, J. Appl. Crystallogr. 39 (2006) 453.
- [42] A.L. Spek, J. Appl. Crystallogr. 36 (2003) 7.
- [43] M. Nardelli, J. Appl. Crystallogr. 28 (1995) 659.
- [44] F.H. Allen, O. Johnson, G.P. Shields, B.R. Smith, M. Towler, J. Appl. Crystallogr. 37 (2004) 335.